Acta virologica **60**: 224 – 233, 2016 doi:10.4149/av_2016_03_224

Yellow mosaic symptom caused by the nuclear shuttle protein gene of mungbean yellow mosaic virus is associated with single-stranded DNA accumulation and mesophyll spread of the virus

B. L. KURUBA, A. P. BUVANI, K. VELUTHAMBI*

Department of Plant Biotechnology, School of Biotechnology, Madurai Kamaraj University, Madurai-625 021, Tamil Nadu, India

Received November 20, 2015; accepted December 9, 2015

Summary. – Mungbean yellow mosaic virus-[India:Vigna] (MYMV-[IN:Vig]), a blackgram isolate of MYMV, causes yellow mosaic disease in blackgram and mungbean. Two variable DNA-B components, KA22 and KA27, cause distinct symptoms in blackgram [*V. mungo* (L.) Hepper] with the same DNA-A component. KA22 + DNA-A-agroinoculated blackgram plants displayed yellow mosaic symptom and accumulated high levels of viral single-stranded (ss) DNA. KA27 + DNA-A-agroinoculated blackgram plants displayed severe stunting symptom and accumulated very low levels of viral ssDNA. However, in mungbean [*V. radiata* (L.) Wilczek], KA27 + DNA-A caused yellow mosaic symptom and a high level of viral ssDNA accumulated. Swapping of KA27 DNA-B with the nuclear shuttle protein gene (*NSP*) of KA22 DNA-B (KA27xKA22 *NSP*) caused yellow mosaic symptom in blackgram, suggesting that KA22 *NSP* is the determinant of yellow mosaic symptom. Interestingly, KA27xKA22 *NSP*-infected blackgram plants accumulated high levels of viral ssDNA, comparable to that of KA22 DNA-B infection, suggesting that the KA22 *NSP* is responsible for accumulation of high levels of viral ssDNA. MYMV distribution was studied in blackgram and mungbean plants by leaf tissue hybridization, which showed mesophyll spread of the virus in KA22-infected blackgram leaflets and in KA27-infected mungbean leaflets, both of which displayed yellow mosaic symptom. However, the virus did not accumulate in the mesophyll in the case of KA27-infected blackgram leaflets. Interestingly, the swapped KA27xKA22 *NSP*-infected blackgram leaflets showed mesophyll accumulation of the virus, suggesting that KA22 *NSP* determines its mesophyll spread.

Keywords: agroinoculation; blackgram; tissue tropism; single-stranded DNA; nuclear shuttle protein; leaf tissue hybridization

Introduction

Mungbean yellow mosaic virus (MYMV) is a geminivirus that infects many pulse crops such as mungbean, blackgram, soybean, mothbean and pigeonpea and causes an annual yield loss of about US $ 300 million (Varma and Malathi, 2003). MYMV is a bipartite begomovirus with two DNA components, DNA-A and DNA-B of 2.7 to 2.8-kb. DNA-A encodes proteins involved in replication, transcriptional activation of viral genes, suppression of siRNA-mediated plant defense and encapsidation of viral genome. DNA-B encodes two movement proteins, nuclear shuttle protein (NSP) and movement protein (MP). NSP is involved in the intracellular trafficking of viral DNA between the nucleus and the cytoplasm, whereas MP controls the cell-to-cell movement of the virus (Hanley-Bowdoin *et al*., 2013). NSP interacts with several host factors both in the nucleus and in the cytoplasm during the process of viral DNA trafficking. NSP interacts with host proteins such as nuclear shuttle protein interactor in *Arabidopsis thaliana* (*At*NSI) to shuttle the viral

*Corresponding author. E-mail: kveluthambi@rediffmail.com; phone: +91-452-2458683.

Abbreviations: dpi = days post infection; MP = movement protein; MYMV = mungbean yellow mosaic virus; NSP = nuclear shuttle protein; ssDNA = single-stranded DNA; SqLCV = Squash leaf curl virus; TGMV = tomato golden mosaic virus

DNA between the nucleus and the cytoplasm (McGarry *et al.*, 2003). Interaction of NSP and *At*NSI is direct and results in the acetylation of viral coat protein. This activity is important for NSP to displace coat protein and to bind ssDNA to export it from the nucleus. NSP-*At*NSI interaction also plays an important role in bipartite geminivirus pathogenicity and infectivity (Carvalho and Lazarowitz, 2004). NSP interacts with a cytosolic GTPase that facilitates the release of viral DNA-NSP complex from the nuclear pores to the cytoplasm (Carvalho *et al.*, 2008a).

NSP interacts with an *Arabidopsis* transmembrane receptor kinase designated as NSP-interacting kinase, NIK (Fontes *et al.*, 2004). Upon geminivirus infection, NIK gets activated by autophosphorylation of the threonine residue at the position 474 (Carvalho *et al.*, 2008b; Rocha *et al.*, 2008; Santos *et al.*, 2009). NIK activation leads to phosphorylation of the ribosomal protein L10 (RPL10) and promotes its translocation to the nucleus, where it interacts with LIMYB (L10 INTERACTING MYB-DOMAIN CONTAINING PROTEIN) and represses translation-related genes. Repression of translation of both host and begomoviral mRNAs enhances tolerance to begomovirus (Carvalho *et al.*, 2008b; Zorzatto *et al.*, 2015). Binding of NSP to the kinase domain of NIK inhibits the kinase activity, resulting in the suppression of NIK-mediated antiviral defense response.

NSP was also shown to interact with a proline-rich extensin-like receptor kinase-like protein from *Arabidopsis,* which is referred to as NSP-associated kinase (NsAK). NsAK acts as a positive contributor for geminivirus infection and is also involved in the regulation of NSP function (Florentino *et al.*, 2006). Histone H3, a host nuclear protein, interacts with *Bean dwarf mosaic virus* (BDMV) NSP and MP and forms a movement-competent nucleoprotein complex with the viral DNA. The role of histone H3 in this process may be in the initial packaging and compaction of viral DNA into a form that can be trafficked through the nuclear pore complex (Zhou *et al.*, 2011).

NSPs of some geminiviruses also function as avirulence (avr) determinants. BDMV NSP induces hypersensitive response in *Phaseolus vulgaris* (Garrido-Ramirez *et al.*, 2000; Zhou *et al.*, 2007) and NSP of *Tomato leaf curl New Delhi virus* (ToLCNDV) induces hypersensitive response in *Nicotiana tabacum* and *Lycopersicon esculentum* (Hussain *et al.*, 2005). NSPs of ToLCNDV (Hussain *et al.*, 2005) and MYMV (Mahajan *et al.*, 2011) were shown to be the symptom determinants in *Nicotiana benthamiana* and *Vigna mungo*, respectively.

Mungbean yellow mosaic virus-[India:Vigna] (MYMV-[IN:Vig]), a blackgram isolate of MYMV, has five variable DNA-B components and one DNA-A component (Karthikeyan *et al.*, 2004). Of the five DNA-B components, KA22 DNA-B and KA27 DNA-B caused distinctly different symptoms upon agroinoculation of blackgram (Balaji *et al.*, 2004). DNA-A + KA22 DNA-B partial dimers caused typical yellow mosaic symptom, whereas DNA-A + KA27 DNA-B caused severe stunting symptom. Swapping of KA27 DNA-B with KA22 *NSP* + C-terminus of MP resulted in the appearance of yellow mosaic symptom typical of KA22 DNA-B suggesting that *NSP* is the major symptom determinant of MYMV DNA-B (Mahajan *et al.*, 2011). The C-terminal end of MP has been reported to influence symptom development in *Tomato mottle virus* (ToMoV) (Duan *et al.*, 1997), *Squash leaf curl virus* (SqLCV) (Pascal *et al.*, 1993) and *Tomato golden mosaic virus* (TGMV) (Saunders *et al.*, 2001). Therefore, we investigated whether the C-terminal 41-amino acids of KA22 MP influenced yellow mosaic symptom development. Here, we report that only KA22 *NSP* but not the C-terminal portion of KA22 MP is responsible for yellow mosaic symptom development. We also report that the *NSP* of KA22 DNA-B is responsible for the accumulation of high levels of viral ssDNA, which may be linked to the mesophyll spread of the virus and development of yellow mosaic symptom.

Materials and Methods

Plant material, viral isolates and plasmid clones. Seeds of blackgram [*V. mungo* (L.) Hepper] cv. CO-5 and mungbean [*Vigna radiata* (L.) Wilczek] cv. CO-4 (obtained from Tamil Nadu Agricultural University, Coimbatore, India) were surface sterilized with 1 % [*w*/*v*] Bavistin (BASF India Ltd., Mumbai, India) + 2–3 drops of Tween 20 for 30 min, 70% [*v*/*v*] ethanol for 5 min, sodium hypochlorite (commercial grade, 4% active chlorine) for 5 min and 0.1% [*w*/*v*] mercuric chloride for 5 min. Treated seeds were rinsed five times with sterile distilled water. Surface sterilized seeds were kept overnight in dark at 25°C ± 2°C in a petridish with a wet Whatman No.1 filter disc.

Accession numbers of DNA-A and two DNA-Bs of MYMV-[IN:Vig] in EMBL/GenBank are as follows: DNA-A KA30, AJ132575; DNA-B KA22, AJ132574; DNA-B KA27, AF262064. All viral DNA components were cloned from field-infected *V. mungo* plants (Karthikeyan *et al.*, 2004). Binary plasmids harboring MYMV-[IN:Vig] partial dimers and the *Agrobacterium tumefaciens* strains harboring the partial dimers used in this study are listed in Table 1.

Agroinoculation. One *A. tumefaciens* strain harboring partial dimer clones of both DNA-A and DNA-B was used for agroinoculation (Jacob *et al.*, 2003). *A. tumefaciens* was grown in AB minimal medium (pH 7.0) (Chilton *et al.*, 1974) with appropriate antibiotics in a shaker at 28°C to 1.0 O.D. at 600 nm. *A. tumefaciens* culture was centrifuged and bacteria were suspended in an equal volume of AB minimal medium (pH 5.6) with 100 μM acetosyringone (Aldrich Chemicals Company, St. Louis, USA). Seed coat was removed from the overnight germinated blackgram seeds and the hypocotyl region was pricked four times with a sterile 30 G hypodermic needle. The seeds were immediately immersed in the *A. tumefaciens* culture.

Table 1. Binary vectors harboring the partial dimers of MYMV-[IN:Vig] DNA-A and DNA-B (KA22 and KA27)

Name of the binary plasmid	Description	*A. tumefaciens* recipient strains	Reference
pGA1.9A[a]	A partial dimer of MYMV DNA-A in pGA472 (An *et al.*, 1985).	Ach5	Jacob *et al.* (2003)
pPZP1.9A	A partial dimer of MYMV DNA-A in pPZP201 (Hajdukiewicz *et al.*, 1994).	C58	Jacob *et al.* (2003)
pPZP1.9B22	A partial dimer of MYMV KA22 DNA-B in pPZP201.	Ach5	Jacob *et al.* (2003)
pGA1.5B27	A partial dimer of MYMV KA27 DNA-B in pGA472.	C58	Balaji *et al.* (2004)
pPZP1.7KA27x KA22 *NSP*+*MP*-CT	A partial dimer of chimeric KA27 DNA-B, into which the KA22 *NSP* was swapped along with KA22 *MP*-C-terminal portion.	Ach5	Mahajan *et al.* (2011)
pPZP1.7KA27x KA22 *NSP*	A partial dimer of chimeric KA27 DNA-B, into which the KA22 *NSP* was swapped.	Ach5	This study

[a]The extent of duplication of the MYMV genome in the partial dimer is denoted in the name of the plasmid. For example, pGA1.9A means that 0.9 portion of DNA A is duplicated in the partial dimer.

Infection was carried out overnight at 25°C. Agroinoculated seedlings were washed twice with sterile distilled water and sown in pots containing 1:1 mixture of autoclaved sand and vermiculite. The seedlings were maintained in a growth chamber set at 25°C with 16/8 h light/dark regimen. Symptoms were monitored periodically and 'top crop' (terminal buds and young leaves) (Mahajan *et al.*, 2011) from five replicate plants was collected 30 days post agroinoculation (dpi) for DNA extraction.

DNA extraction, S1 nuclease treatment and Southern blot analysis. Total DNA from agroinoculated plants was extracted as described by Porebski *et al.* (1997). DNA concentration was estimated using the Hoechst dye 33258 in a DNA fluorometer. For S1 nuclease treatment, 1.0 µg of total plant DNA and 1.2 µg of denatured calf thymus DNA were mixed and digested for 30 min at 37°C with 1.5 units of S1 nuclease (Pharmacia, Uppsala, Sweden) in 5 µl of sodium acetate buffer (50 mmol/l, pH 4.6) containing 280 mmol/l NaCl and 4.5 mmol/l $ZnSO_4$. The reaction was stopped by adding 5 µl of 0.1 mol/l EDTA (pH 8.0). One microgram of total plant DNA was electrophoresed in 1% [*w*/*v*] agarose gels in 1x Tris-sodium acetate-EDTA (TNE) buffer (Hong and Stanley, 1996). The gel was stained with ethidium bromide and Southern blotting was done in denaturing and non-denaturing conditions using the nitrocellulose membrane (NCM) (BioTrace™ NT, PALL Life sciences, Pensacola, USA). To perform denaturing Southern blotting, the gel was subjected to alkali-denaturation and neutralization prior to the transfer of DNA onto NCM (Southern, 1975). For performing non-denaturing Southern blotting, the gel was not treated with NaOH prior to transfer to NCM (Stachel *et al.*, 1986). DNA was fixed by baking the membrane at 80°C for 2 hr under vacuum. Hybridization was performed overnight at 65°C in a hybridization oven using [α-^{32}P]dCTP (~ 3000 Ci/mmol, BRIT, Mumbai, India)-labeled probes. The probes were prepared by using the Megaprime™ DNA labeling system (GE Healthcare UK Ltd., Little Chalfont, UK). Post hybridization washes were done three times with 0.3x SSC, 0.1% SDS, 5 mmol/l EDTA at 65°C (each wash for 30 min).

Construction of partial dimer of chimeric KA27 DNA-B swapped with KA22 NSP. A 289-bp fragment of KA27 DNA-B (EMBL/GenBank-AF262064-coordinates 1054 nt to 1343 nt) comprising 138-bp encoding the C-terminal 45-amino acid-portion of KA27 NSP (+ stop codon), 126-bp encoding the C-terminal 41-amino acid-portion of KA27 MP (+ stop codon) and 25-bp intergenic region between KA27 *NSP* and *MP* was PCR-amplified. The forward primer (5'-ACGTTTAAGGATCCTGAGCTTGG-3') had an embedded *Bam*HI (underlined) site. The primer was designed to create a *Bam*H1 site by making a single nucleotide change from A to G at the nucleotide position 1054 in KA27 DNA-B. This did not change the amino acid sequence. A reverse primer (5'-ATTACCGGAGTCGTCTCT AGACC-3') with an embedded *Xba*I (underlined) site was used. pKA27 (a KA27 DNA-B clone) was used as the template for PCR amplification. The amplified 289-bp fragment was confirmed by sequencing and was taken as a *Bam*HI/*Xba*I fragment to exchange with the corresponding portion of the KA22 sequence in pNMM23 (Mahajan *et al.*, 2011) to yield the plasmid pKB11. A 928-bp *Bgl*II/*Xba*I fragment with complete KA27 *MP* and 694-bp *Bgl*II/*Cla*I fragment of KA27 CR were cloned in successive steps into pKB11 to yield the plasmid pIC19HKA27xKA22 *NSP*, which comprises the full-length (2558 bp) chimeric KA27 DNA-B swapped with the KA22 *NSP*. Although the NSP of this clone has N-terminal 211-amino acids of KA22 NSP + C-terminal 45-amino acids of KA27 NSP, we refer this as KA22 NSP in this paper. The partial dimer of KA27xKA22 *NSP* was constructed in the pPZP201 binary vector (Hajdukiewicz *et al.*, 1994) by first cloning a 1896-bp *Cla*I/*Bam*HI fragment of KA27xKA22 *NSP* (0.7-mer of the chimeric KA27 DNA-B). Subsequently, the 2558-bp *Cla*I fragment of unit-length KA27xKA22 *NSP* was cloned to yield the partial dimer clone pPZP1.7KA27xKA22 *NSP* (Fig. 1). pPZP1.7KA27xKA22 *NSP* was mobilized by triparental mating into the *A. tumefaciens* strain Ach5 (pGA1.9A) (Jacob *et al.*, 2003). pGA1.9A harbors the MYMV DNA-A partial dimer. *A. tumefaciens* (pGA1.9A) transconjugants with pPZP1.7KA27xKA22 *NSP* were confirmed by Southern blot analysis.

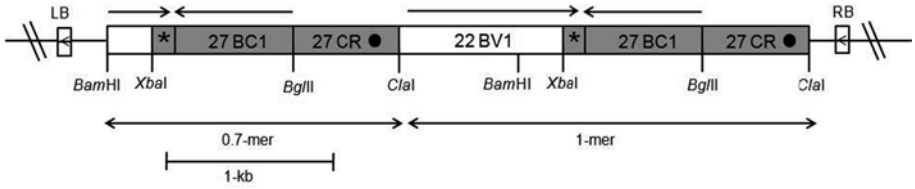

Fig. 1

T-DNA map of the binary vector pPZP1.7KA27xKA22 *NSP* depicting the partial dimer of chimeric KA27 DNA-B swapped with KA22 *NSP*
The sequences derived from KA27 DNA-B are in shaded boxes; those from KA22 DNA-B are in open boxes. Asterisk (*) represents the C-terminal 45-amino acid-portion of KA27 NSP. The directions of the ORFs are indicated by the *arrows* above the boxes. The *double headed arrows* below the boxes indicate the *0.7-mer* (1.9-kb *Cla*I/*Bam*HI fragment) and monomer (*1-mer*) (2.7-kb *Cla*I fragment) portions of the viral DNA. Scale bar in kb (*1-kb*) is indicated. Right T-DNA border (*RB*), left T-DNA border (*LB*) and common region () are indicated.

Leaf tissue hybridization analysis. Leaflets from fully expanded blackgram and mungbean leaves (approximately 0.2 g) were collected from control and agroinoculated plants 45 dpi and treated with 100 ml of 80% [*v*/*v*] ethanol over a boiling waterbath for 10 min. This step was repeated thrice. The leaflet was treated like a DNA-immobilized membrane. The ethanol-treated leaflets were subjected to denaturation and neutralization steps as done in Southern blotting (Southern, 1975). The leaflets were air dried on Whatman No. 1 filter discs for 30 sec. Fixing of the DNA to the leaf tissue was skipped since the DNA is already trapped inside the leaf tissue. The processed leaflets were taken in a hybridization bottle and subjected to prehybridization using 20 ml of prewarmed (65°C) prehybridization solution I (6x SSC, 10x Denhardts solution, 20 mmol/l Tris, pH 7.0) for 12 hr in a hybridization oven at 65°C. The leaflets were then treated with 9 ml of freshly prepared hybridization solution [equal volumes of prehybridization solution I and prehybridization solution II (1 mmol/l Tris, pH 7.0, 5 mmol/l EDTA, 0.5% SDS, 0.75 mg/ml sheared calf thymus DNA)] for 6 hr at 65°C and then subjected to hybridization for 12 hr at 65°C using MYMV DNA-A (without common region) labeled with [α-^{32}P]dCTP (BRIT, Mumbai, India) using Megaprime^{TM} DNA labeling system (Amersham Biosciences Ltd., Little Chalfont, UK). The leaflets were rinsed briefly with 20 ml of prewarmed (65°C) wash solution (0.3x SSC, 0.1% SDS, 5 mmol/l EDTA, pH 7.0). Unhybridized labeled probe was removed from the tissue by three subsequent washes (30 min each) at 65°C using 40 ml of the prewarmed wash solution. Finally, the tissue was rinsed briefly using 2x SSC at room temperature and air dried. Konica Type AX X-ray film was exposed to the hybridized leaf tissue in an exposure cassette with intensifying screen (Amersham Biosciences Ltd., Little Chalfont, UK) and the cassette was left at -70°C.

Results

KA22 NSP alone, not the C-terminal portion of KA22 MP, is the determinant of yellow mosaic symptom

We reported earlier that KA27 DNA-B, swapped with KA22 *NSP* plus C-terminal 41-amino acid-portion of KA22 MP (designated here as KA27xKA22 *NSP*+*MP*-CT) caused yellow mosaic symptom in blackgram (Mahajan *et al.*, 2011), as produced by KA22 DNA-B. In this study, we analyzed whether the KA22 *NSP* or the C-terminal 41-amino acid portion of KA22 MP is responsible for causing the yellow mosaic symptom in blackgram. Evidence for C-terminal end of MP to influence symptom development has been provided for ToMoV (Duan *et al.*, 1997), SqLCV (Pascal *et al.*, 1993) and TGMV (Saunders *et al.*, 2001). A chimeric KA27 DNA-B clone pIC19HKA27xKA22 *NSP* was constructed without the C-terminal portion of KA22 MP. It comprised KA27 DNA-B CR, complete KA27 *MP* and KA22 *NSP* (Fig. 1). The partial dimer of KA27xKA22 *NSP* was constructed in pPZP201 to yield the plasmid pPZP1.7KA27xKA22 *NSP*. Agroinoculation of sprouted blackgram seeds using MYMV DNA-A (pGA1.9A) and KA22 DNA-B (pPZP1.9B22) partial dimer clones (Table 1) produced typical yellow mosaic symptom without reducing the height of plants (Fig. 2a and b), whereas agroinoculation of blackgram with DNA-A (pPZP1.9A) and KA27 DNA-B (pGA1.5B27) partial dimer clones (Table 1) produced severe stunting symptom (Fig. 2a and b). Agroinoculation of blackgram seedlings with DNA-A (pGA1.9A) and chimeric KA27 DNA-B swapped with KA22 *NSP* (pPZP1.7KA27xKA22 *NSP*) partial dimer clones did not produce severe stunting symptom but produced yellow mosaic symptom (Fig. 2a and b). These results suggest that the KA22 *NSP*, but not the C-terminal 41-amino acid-portion of KA22 MP, is responsible for causing yellow mosaic symptom in blackgram.

KA22 NSP is responsible for the accumulation of high levels of viral ssDNA

Plant DNA from the 'top crop' (terminal buds and young leaves) of the agroinoculated blackgram plants was extracted to study the viral DNA accumulation in the infected blackgram plants. Electrophoresis in TNE buffer (Hong and Stanley, 1996) helps in identifying the *oc, lin, sc* and *ss* forms of geminiviral DNA in infected plants. Southern blot

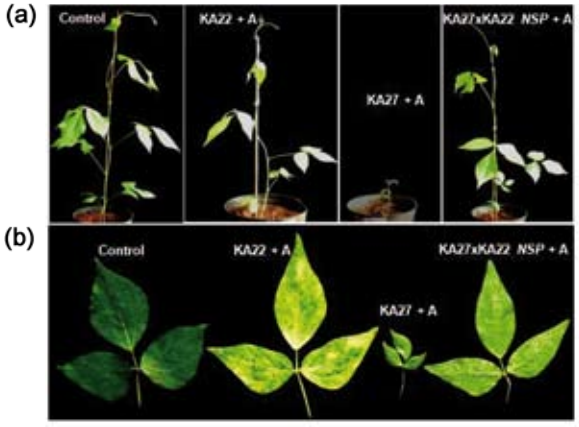

Fig. 2

Agroinoculation of blackgram with chimeric MYMV KA27 DNA-B swapped with the KA22 *NSP* showing yellow mosaic symptom and absence of severe stunting

(a) Blackgram plants and (b) trifoliate leaves of plants mock-inoculated with AB buffer without *Agrobacterium* culture (*Control*), agroinoculated with DNA-A + KA22 DNA-B partial dimers (*KA22 + A*), DNA-A + KA27 DNA-B partial dimers (*KA27 + A*) and DNA-A + KA27xKA22 *NSP* partial dimers (*KA27xKA22 NSP + A*). Pictures were taken 45 dpi.

analysis with the DNA-A probe displayed two major bands moving at the 2.7-kb [comprising open circular (*oc*) or linear (*lin*) dsDNA] and 1.8-kb [comprising supercoiled dsDNA (*sc*) and ssDNA (*ss*)] positions (Fig. 3). The band intensity of DNA-A at the 2.7-kb position was comparable in plants agroinoculated with KA22, KA27, KA27xKA22 *NSP*+*MP*-CT and KA27xKA22 *NSP* (Fig. 3a). But the band intensity of DNA at the 1.8-kb position, which represents supercoiled dsDNA and ssDNA forms, was much lower in KA27-infected plant DNA in comparison to KA22-infected plant DNA. The band intensity of DNA at the 1.8-kb position was comparable in plants infected with KA22, KA27xKA22 *NSP*+*MP*-CT and KA27xKA22 *NSP* (Fig. 3a). The same pattern of viral DNA forms accumulated in two swapping experiments, one in which KA27 DNA-B was swapped with KA22 *NSP*+*MP*-CT and the other in which KA27 DNA-B was swapped with only KA22 *NSP*. These results suggest that the high band intensity of DNA at the 1.8-kb position was contributed by KA22 *NSP* and did not require KA22 MP-CT.

Two approaches were taken to differentiate between ss- and ds-forms of viral DNA at the 1.8-kb position. In the first approach, S1 nuclease, which degrades ssDNA but not dsDNA,

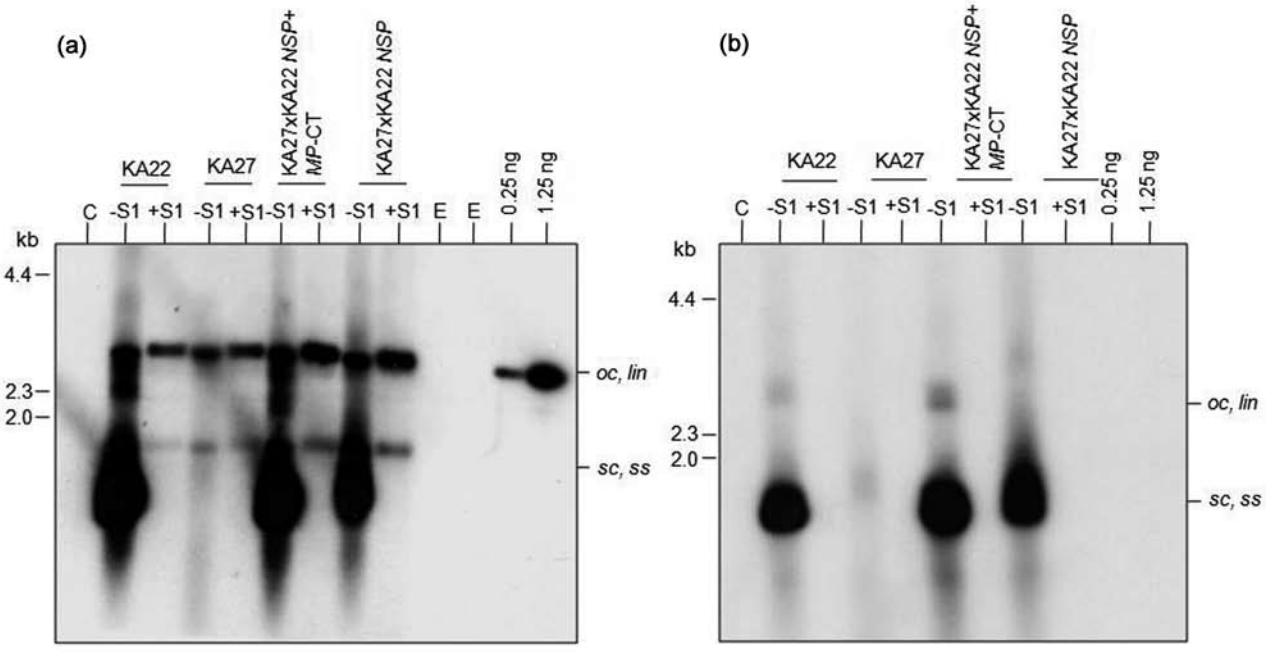

Fig. 3

Southern blot analyses of blackgram plants agroinoculated with swapped KA27xKA22 *NSP*

Undigested DNA (1 µg) was electrophoresed and the blot was probed with [α-^{32}P]dCTP-labeled DNA-A without the common region. Denatured (a) and non-denatured (b) Southern blot analyses were done. (a and b) DNA (1 µg) from mock-inoculated blackgram plants (c), agroinoculated with KA22 DNA-B + A (*KA22*), KA27 DNA-B + A (*KA27*), KA27xKA22 *NSP*+*MP*-CT + A (*KA27xKA22 NSP*+*MP-CT*) and KA27xKA22 *NSP* + A (*KA27xKA22 NSP*) partial dimers were analyzed. A 1.2-kb *Bam*HI fragment of pKA30 (a DNA-A clone) was used as the probe. pKA30 (*0.25 ng* and *1.25 ng*) digested with *Pst*I was used as the positive control. DNA samples (1 µg) subjected to S1 nuclease treatment (+*S1*) and samples without S1 nuclease treatment (-*S1*) were loaded. Empty lane, no DNA loaded (*E*), open circular double-stranded DNA (*oc*), linear double-stranded DNA (*lin*), supercoiled double-stranded DNA (*sc*), single-stranded DNA (*ss*).

was used to digest plant DNA prior to electrophoresis. In the second approach, the DNA from virus-infected plants was subjected to non-denatured Southern blotting (Stachel *et al.*, 1986). Since nitrocellulose membrane was used in the blotting experiments, only ssDNA will bind to the membrane under non-denatured blotting conditions. In contrast, in routine Southern blotting, in which the DNA is denatured, both ssDNA and dsDNA forms will bind to the nitrocellulose membrane.

In the denatured blot shown in Fig. 3a, bulk of the DNA in the 1.8-kb position was absent in +S1 lanes indicating its single-stranded nature. The ssDNA form, interestingly, was low or absent in KA27-infected plants. As expected, only the signal for ssDNA at the 1.8-kb position was detected in the non-denatured blot shown in Fig. 3b. This band was conspicuously absent in the lane of KA27 DNA-B-infected plants. Both experimental approaches clearly showed that ssDNA form of the virus predominantly accumulated in KA22 DNA-B-infected plants and not in KA27 DNA-B-infected plants. Very interestingly, swapping of KA27 DNA-B with KA22 *NSP* caused the accumulation of viral ssDNA. Thus, swapping of KA27 DNA-B with KA22 *NSP* altered the severe stunting symptom to yellow mosaic symptom and brought about the accumulation of viral ssDNA. Based on the above result, we propose that there is a good correlation between yellow mosaic symptom and accumulation of high levels of viral ssDNA as displayed by KA22- and KA27xKA22 *NSP*-infected blackgram plants. To further confirm this correlation, we analysed KA27-infected mungbean (*V. radiata*) plants, which showed yellow mosaic symptom upon agroinoculation with MYMV DNA-A and KA27 DNA-B partial dimers (Balaji *et al.*, 2004). Southern blot analysis (denatured) of the DNA extracted from the 'top crop' (terminal buds and young leaves) of the KA27-infected mungbean plants with the DNA-A probe displayed two major bands moving at the 2.7-kb and 1.8-kb positions (Fig. 4a). The band intensity of the DNA at the 1.8-kb position which represents supercoiled dsDNA and ssDNA forms, was high, which was comparable to that of KA22- and KA27xKA22 *NSP*-infected blackgram plants. The 1.8-kb band was present in the non-denatured Southern blot (Fig. 4b) and disappeared upon S1 nuclease treatment confirming its ssDNA nature. Thus, a good correlation between yellow mosaic symptom and high level of viral ssDNA accumulation was seen in both blackgram and mungbean plants infected with MYMV.

Yellow mosaic symptom in blackgram (V. mungo) and mungbean (V. radiata) is associated with mesophyll spread of MYMV DNA: NSP is responsible for MYMV spread to mesophyll

To study the distribution of virus in the leaves of MYMV-infected blackgram and mungbean plants, a method of 'leaf

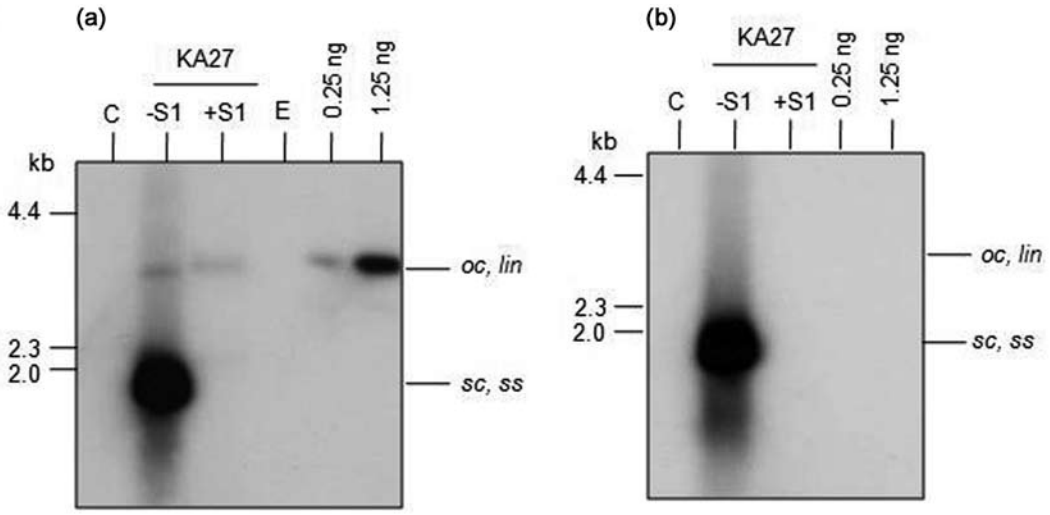

Fig. 4

Southern blot analyses of KA27 agroinoculated mungbean plants

Undigested DNA (1 µg) was electrophoresed, subjected to denatured (a) or non-denatured (b) Southern blotting, and the blot was probed with [α-^{32}P] dCTP-labeled DNA-A without the common region. (a and b) DNA (1 µg) from mock-inoculated mungbean plants (*C*) and KA27 DNA-B + A- agroinoculated plants (*KA27*) were analysed. A 1.2-kb *Bam*HI fragment of pKA30 (a DNA-A clone), without the common region, labeled with [α-^{32}P]dCTP was used as the probe. pKA30 (*0.25 ng* and *1.25 ng*) digested with *Pst*I was used as the positive control. DNA samples (1 µg) subjected to S1 nuclease treatment (*+S1*) and samples without S1 nuclease treatment (*-S1*) were loaded. Empty lane, no DNA loaded (*E*), open circular double-stranded DNA (*oc*), linear double-stranded DNA (*lin*), supercoiled double-stranded DNA (*sc*), single-stranded DNA (*ss*).

tissue hybridization' was used. After extraction of low molecular weight molecules with 80 % ethanol, the leaf, which retained DNA, was treated like a DNA-bound membrane and used for hybridization. Young, fully expanded leaflets of KA22-infected blackgram plants, KA27-infected blackgram plants, KA27-infected mungbean plants and mock-inoculated blackgram and mungbean plants were processed with 80% alcohol as described in Materials and methods and hybridized with [α-^{32}P]dCTP-labeled DNA-A without common the region. The leaflets from mock-inoculated blackgram and mungbean plants did not show any hybridization to the probe (Fig. 5a and f), whereas KA22-infected blackgram (Fig. 5b) and KA27-infected mungbean leaflets (Fig. 5g) showed intense hybridization throughout the leaflet. KA27-infected blackgram leaflet showed very weak hybridization (Fig. 5c). These results suggest mesophyll spread of MYMV in KA22-infected blackgram plants and KA27-infected mungbean plants. Although KA27 DNA-B-infected blackgram leaves accumulated MYMV dsDNA, as analyzed by Southern blotting (Fig. 3a), only very weak hybridization signal was noticed in leaf tissue hybridization. This may be due to vascular limitation of the virus and absence of mesophyll spread. It is interesting to note that KA27 DNA-B, which caused yellow mosaic symptom in mungbean (Balaji *et al.*, 2004) caused mesophyll spread of MYMV.

The yellow mosaic symptom exhibited by the swapped KA27xKA22 *NSP*-infected blackgram plants prompted us to study whether KA22 *NSP* mediated the virus spread to mesophyll in these plants. Young, fully expanded blackgram leaflets from plants infected with swapped KA27xKA22 *NSP*+*MP*-CT and swapped KA27xKA22 *NSP* were taken 45 dpi for leaf tissue hybridization analysis. Interestingly, leaflets of blackgram plants infected with KA27xKA22 *NSP*+*MP*-CT (Fig. 5d) and KA27xKA22 *NSP* (Fig. 5e) showed hybridization throughout the lamina. The extent of spread and intensity of hybridization were comparable to those seen in KA22-infected blackgram leaflets (Fig. 5b). Thus, swapping of KA22 *NSP* into KA27 DNA-B is sufficient to cause mesophyll spread of the virus and change the severe stunting symptom of KA27 DNA-B to the yellow mosaic symptom of KA22 DNA-B.

Discussion

Our previous work with the MYMV KA27 DNA-B swapped with KA22 *NSP*+*MP*-CT (Mahajan *et al.*, 2011)

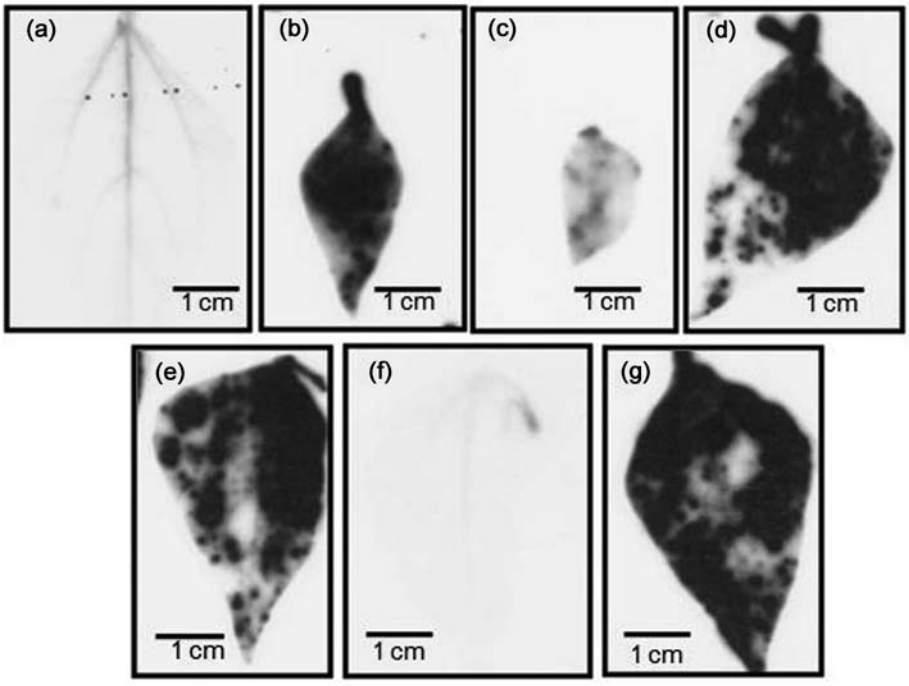

Fig. 5

Leaf tissue hybridization analysis of KA22-, KA27-, swapped KA27xKA22 *NSP*+*MP*-CT-and swapped KA27xKA22 *NSP*-agroinoculated blackgram plants and KA27-agroinoculated mungbean plants

Fully expanded mock-inoculated (*a*) and KA22 DNA-B + A-(*b*), KA27 DNA-B + A-(*c*), swapped KA27xKA22 *NSP*+*MP*-CT + A-(*d*) and swapped KA27xKA22 *NSP* + A-(*e*) agroinoculated blackgram plant leaflets collected 45 dpi were used. Mock-inoculated (*f*) and KA27 DNA-B + A-(*g*) agroinoculated mungbean plant leaflets collected 45 dpi were used. A 1.2-kb *Bam*HI fragment of pKA30 (a DNA-A clone), without the common region, labeled with [α-^{32}P]dCTP was used as the probe. Scale bar in cm (*1cm*) is indicated.

showed that the symptom changed in blackgram from severe stunting of KA27 DNA-B to the yellow mosaic symptom of KA22 DNA-B. Although it was clear that *NSP* was the symptom determinant, the impact of the C-terminal 41-amino acids of KA22 MP on symptom development could not be ruled out. The reports on ToMoV (Duan *et al*., 1997), SqLCV (Pascal *et al*., 1993) and TGMV (Saunders *et al*., 2001) suggest that the C-terminus of MP of the respective geminiviruses influenced symptom development in the infected plants. In the agroinoculation analysis reported here with the swapped MYMV KA27xKA22 *NSP,* without the C-terminal part of KA22 MP, clear yellow mosaic symptom was observed. Thus, KA22 *NSP* is the determinant of the yellow mosaic symptom in blackgram plants.

Two experimental approaches, S1 nuclease treatment of infected plant DNA prior to electrophoresis and non-denatured Southern blotting, revealed that blackgram plants, which displayed yellow mosaic symptom upon infection with KA22 DNA-B, KA27xKA22 *NSP+MP*-CT or KA27xKA22 *NSP,* accumulated high levels of viral ssDNA. In contrast, KA27 DNA-B-infected blackgram plants, which displayed severe stunting symptom, accumulated very little or no viral ssDNA. This is a new report wherein we show that geminiviral *NSP* determines whether ss- or dsDNA forms of a geminivirus accumulate in infected plants.

The agroinoculation studies showed that plant factors also govern symptom development. KA27 DNA-B, which caused severe stunting in blackgram, caused yellow mosaic symptom in mungbean. Interestingly, KA27 DNA-B-infected mungbean plants accumulated high levels of viral ssDNA. It is interesting to note that there is good correlation between viral ssDNA accumulation and development of yellow mosaic symptom in both blackgram and mungbean.

The tissue tropism of mono- and bipartite geminiviruses has been investigated using electron microscopy and *in situ* hybridization techniques in previous reports. Monopartite and some bipartite begomoviruses such as *Tomato yellow leaf curl virus* (TYLCV, Morilla *et al*., 2004), abutilon mosaic virus (AbMV) and sida micrantha mosaic virus (SimMV) (Wege *et al*., 2001), bean golden mosaic virus (BGMV, Carr and Kim, 1983) and SqLCV (Hoefert, 1987) are phloem-limited. However, some bipartite begomoviruses such as *African cassava mosaic virus* (ACMV), BDMV and TGMV invade mesophyll as well as epidermal cells (Sudarshana *et al*., 1998; Wege *et al*., 2001). We used here a simple procedure of leaf tissue hybridization, a modified Southern blotting procedure, in which 80 % ethanol-treated leaflet was used like a DNA-immobilized membrane for hybridization. This method picked up hybridization to the geminivirus that accumulated in the mesophyll. KA22 DNA-B-, KA27xKA22 *NSP+MP*-CT- or KA27xKA22 *NSP*-infected blackgram plants and KA27 DNA-B-infected mungbean plants showed intense hybridization to MYMV DNA-A all over the leaf lamina. It is to be noted that all these viral infections caused yellow mosaic symptom and directed the accumulation of viral ssDNA. KA27 DNA-B-infected blackgram plants, which displayed severe stunting, did not show hybridization in the leaf lamina. Denatured Southern blotting of KA27 DNA-B-infected blackgram plant DNA using the nitrocellulose membrane showed accumulation of viral dsDNA (Fig. 3a). Probably because these DNA molecules are in the deeper layers of the phloem tissue, hybridization to the probe may not have been effective in leaf tissue blots. On this basis, we propose that MYMV dsDNA does not spread to mesophyll, whereas MYMV ssDNA spreads to the mesophyll tissue. This hypothesis is further strengthened by the fact that, KA27 DNA-B infection in mungbean, which generates viral ssDNA (Fig. 4) and causes yellow mosaic symptom (Balaji *et al*., 2004), also enables mesophyll accumulation of the virus (Fig. 5g).

The tropism of viral movement may influence symptom development. Wege *et al.* (2001) demonstrated that ACMV and TGMV infected phloem tissue in the initial stage of infection and caused mild symptoms in *N. benthamiana.* In the later stages, ACMV and TGMV infected all the tissues causing severe symptoms in *N. benthamiana*. In KA27-infected blackgram plants, the virus does not spread to mesophyll and yellow mosaic symptom is not caused. However, in KA22-infected blackgram plants, the virus spreads to the mesophyll cells and causes yellow mosaic symptom. Since the developmental stage of the host plant can affect the tissue tropism in begomoviruses (Wang *et al*., 1996), we took the leaflets from the virus-infected blackgram and mungbean plants at the same time post infection (45 dpi).

Morra and Petty (2000) studied the viral components that are important for mesophyll spread of TGMV and phloem restriction of BGMV. By *in situ* hybridization analysis of TGMV/BGMV chimeras it was shown that the TGMV components, *BRi* (the non-coding sequence upstream of the BV1 ORF) + AL23 (AC2 and AC3 ORFs together) or *BRi* + BL1/BR1 (BC1 and BV1 ORFs together), altered the phloem-limited BGMV to become a mesophyll invading virus. Qin and Petty (2001) further delineated the cis-acting elements in *BRi,* which are required for mesophyll invasion, by constructing BGMV-based hybrid viruses with different parts of TGMV *BRi.* This study revealed that a 52-bp region of TGMV *BRi* directs the mesophyll spread of the phloem-restricted BGMV in *N. benthamiana* plants. Based on the observation of intense hybridization to MYMV DNA-A all over the leaf lamina of KA27xKA22 *NSP+MP*-CT- and KA27xKA22 *NSP*-infected blackgram plants we propose that KA22 *NSP* is responsible for the mesophyll spread of *MYMV.*

This report shows that MYMV KA22 *NSP*, a symptom determinant, also regulates viral ssDNA accumulation and controls mesophyll spread of the virus. This is the first re-

port that establishes a link between geminivirus symptom development, viral ssDNA accumulation and mesophyll spread of the virus.

Acknowledgements. We thank Dr K. Dharmalingam, School of Biotechnology, Madurai Kamaraj University, for his permission to use the radioisotope facility. We thank the scientists at Tamil Nadu Agricultural University, Coimbatore, Tamil Nadu for providing *Vigna mungo* and *Vigna radiata* seeds. Bhagya Lakshmi Kuruba acknowledges the Department of Biotechnology, Government of India for granting DBT JRF/SRF fellowship. University Grants Commission BSR Faculty Fellowship to K. Veluthambi [No. F. 18-1 (61)/2014 (BSR)] is acknowledged.

References

An G, Watson BD, Stachel S, Gordon MP, Nester EW (1985): New cloning vehicles for transformation of higher plants. EMBO J. 4, 277–284.

Balaji V, Vanitharani R, Karthikeyan AS, Anbalagan S, Veluthambi K (2004): Infectivity analysis of two variable DNA B components of Mungbean yellow mosaic virus-Vigna in Vigna mungo and Vigna radiata. J. Biosci. 29, 297–308. http://dx.doi.org/10.1007/BF02702612

Carr RJ, Kim KS (1983): Evidence that Bean golden mosaic virus invades non-phloem tissue in double infections with Tobacco mosaic virus. J. Gen. Virol. 64, 2489–2492. http://dx.doi.org/10.1099/0022-1317-64-11-2489

Carvalho CM, Fontenelle MR, Florentino LH, Santos AA, Zerbini FM, Fontes EPB (2008a): A novel nucleocytoplasmic traffic GTPase identified as a functional target of the bipartite geminivirus nuclear shuttle protein. Plant J. 55, 869–880. http://dx.doi.org/10.1111/j.1365-313X.2008.03556.x

Carvalho CM, Santos AA, Pires SR, Rocha CS, Saraiva DI, Machado JPB, Mattos EC, Fietto LG, Fontes EPB (2008b): Regulated nuclear trafficking of rpL10A mediated by NIK1 represents a defense strategy of plant cells against virus. PLoS Pathog. 4, e1000247. http://dx.doi.org/10.1371/journal.ppat.1000247

Carvalho MF, Lazarowitz SG (2004): Interaction of the movement protein NSP and the Arabidopsis acetyltransferase AtNSI is necessary for Cabbage leaf curl geminivirus infection and pathogenicity. J. Virol. 78, 11161–11171. http://dx.doi.org/10.1128/JVI.78.20.11161-11171.2004

Chilton M, Currier TC, Farrand SK, Bendich AJ, Gordon MP, Nester EW (1974): Agrobacterium tumefaciens DNA and PS8 bacteriophage DNA not detected in crown gall tumors. Proc. Natl. Acad. Sci. USA 71, 3672–3676. http://dx.doi.org/10.1073/pnas.71.9.3672

Duan YP, Powell CA, Webb SE, Purcifull DE, Hiebert E (1997): Geminivirus resistance in transgenic tobacco expressing mutated BC1 protein. Mol. Plant-Microbe Interact. 10, 617–623. http://dx.doi.org/10.1094/MPMI.1997.10.5.617

Florentino LH, Santos AA, Fontenelle MR, Pinheiro GL, Zerbini FM, Baracat-Pereira MC, Fontes EPB (2006): A PERK-like receptor kinase interacts with the geminivirus nuclear shuttle protein and potentiates viral infection. J. Virol. 80, 6648–6656. http://dx.doi.org/10.1128/JVI.00173-06

Fontes EPB, Santos AA, Luz DF, Waclawovsky AJ, Chory J (2004): The geminivirus nuclear shuttle protein is a virulence factor that suppresses transmembrane receptor kinase activity. Genes Dev. 18, 2545–2556. http://dx.doi.org/10.1101/gad.1245904

Garrido-Ramirez ER, Sudarshana MR, Lucas WJ, Gilbertson RL (2000): Bean dwarf mosaic virus BV1 protein is a determinant of the hypersensitive response and avirulence in Phaseolus vulgaris. Mol. Plant-Microbe Interact. 13, 1184–1194. http://dx.doi.org/10.1094/MPMI.2000.13.11.1184

Hajdukiewicz P, Svab Z, Maliga P (1994): The small, versatile pPZP family of Agrobacterium binary vectors for plant transformation. Plant Mol. Biol. 25, 989–994. http://dx.doi.org/10.1007/BF00014672

Hanley-Bowdoin L, Bejarano ER, Robertson D, Mansoor S (2013): Geminiviruses: masters at redirecting and reprogramming plant processes. Nat. Rev. Microbiol. 11, 777–788. http://dx.doi.org/10.1038/nrmicro3117

Hoefert LL (1987): Association of Squash leaf curl virus with nuclei of squash vascular cells. Phytopathology 77, 1596–1600. http://dx.doi.org/10.1094/Phyto-77-1596

Hong Y, Stanley J (1996): Virus resistance in Nicotiana benthamiana conferred by African cassava mosaic virus replication-associated protein (AC1) transgene. Mol. Plant-Microbe Interact. 9, 219–225. http://dx.doi.org/10.1094/MPMI-9-0219

Hussain M, Mansoor S, Iram S, Fatima AN, Zafar Y (2005): The nuclear shuttle protein of Tomato leaf curl New Delhi virus is a pathogenicity determinant. J. Virol. 79, 4434-4439. http://dx.doi.org/10.1128/JVI.79.7.4434-4439.2005

Jacob SS, Vanitharani R, Karthikeyan AS, Chinchore Y, Thillaichidambaram P, Veluthambi K (2003): Mungbean yellow mosaic virus-Vi Agroinfection by codelivery of DNA A and DNA B from one Agrobacterium strain. Plant Dis. 87, 247–251. http://dx.doi.org/10.1094/PDIS.2003.87.3.247

Karthikeyan AS, Vanitharani R, Balaji V, Anuradha S, Thillaichidambaram P, Shivaprasad PV, Parameswari C, Balamani V, Saminathan M, Veluthambi K (2004): Analysis of an isolate of Mungbean yellow mosaic virus (MYMV) with a highly variable DNA B component. Arch. Virol. 149, 1643–1652. http://dx.doi.org/10.1007/s00705-004-0313-z

Mahajan N, Parameswari C, Veluthambi K (2011): Severe stunting in blackgram caused by the Mungbean yellow mosaic virus (MYMV) KA27 DNA B component is ameliorated by co-infection or post-infection with the KA22 DNA B: MYMV nuclear shuttle protein is the symptom determinant. Virus Res. 157, 25–34. http://dx.doi.org/10.1016/j.virusres.2011.01.013

McGarry RC, Barron YD, Carvalho MF, Hill JE, Gold D, Cheung E, Kraus WL, Lazarowitz SG, (2003): A novel Arabidopsis acetyltransferase interacts with the geminivirus move-

ment protein NSP. Plant Cell 15, 1605–1618. http://dx.doi.org/10.1105/tpc.012120

Morilla G, Krenz B, Jeske H, Bejarano ER, Wege C (2004): Tete a tete of Tomato yellow leaf curl virus and Tomato yellow leaf curl Sardinia virus in single nuclei. J. Virol. 78, 10715–10723. http://dx.doi.org/10.1128/JVI.78.19.10715-10723.2004

Morra MR., Petty ITD (2000): Tissue specificity of geminivirus infection is genetically determined. Plant Cell 12, 2259–2270. http://dx.doi.org/10.1105/tpc.12.11.2259

Pascal E, Goodlove PE, Wu LC, Lazarowitz SG (1993): Transgenic tobacco plants expressing the geminivirus BL1 protein exhibit symptoms of viral disease. Plant Cell 5, 795–807. http://dx.doi.org/10.1105/tpc.5.7.795

Porebski S, Bailey LG, Baum BR (1997): Modification of a CTAB DNA extraction protocol for plants containing high polysaccharide and polyphenol components. Plant Mol. Biol. Rep. 15, 8–15. http://dx.doi.org/10.1007/BF02772108

Qin Y, Petty ITD (2001): Genetic analysis of bipartite geminivirus tissue tropism. Virology 291, 311–323. http://dx.doi.org/10.1006/viro.2001.1205

Rocha CS, Santos AA, Machado JPB, Fontes EPB (2008): The ribosomal protein L10/QM-like protein is a component of the NIK-mediated antiviral signaling. Virolgy 380, 165–169. http://dx.doi.org/10.1016/j.virol.2008.08.005

Santos AA, Carvalho CM, Florentino LH, Ramos HJO, Fontes EPB (2009): Conserved threonine residues within the A-loop of the receptor NIK differentially regulate the kinase function required for antiviral signaling. PLoS ONE 4, e5781. http://dx.doi.org/10.1371/journal.pone.0005781

Saunders K, Wege C, Veluthambi K, Jeske H, Stanley J (2001): The distinct disease phenotypes of the common and yellow vein strains of Tomato golden mosaic virus are determined by nucleotide differences in the 3'-terminal region of the gene encoding the movement protein. J. Gen. Virol. 82, 45–51. http://dx.doi.org/10.1099/0022-1317-82-1-45

Southern EM (1975): Detection of specific sequences among DNA fragments separated by gel electrophoresis. J. Mol. Biol. 98, 503–517. http://dx.doi.org/10.1016/S0022-2836-(75)80083-0

Stachel SE, Timmermans B, Zambryski P (1986): Generation of single-stranded T-DNA molecules during the initial stages of T-DNA transfer from Agrobacterium tumefaciens to plant cells. Nature 322, 706–712. http://dx.doi.org/10.1038/322706a0

Sudharshana MR, Wang HL, Lucas WJ, Gilbertson RL (1998): Dynamics of Bean dwarf mosaic geminivirus cell-to-cell and long-distance movement in Phaseolus vulgaris revealed, using the green fluorescent protein. Mol. Plant-Microbe Interact. 11, 277–291. http://dx.doi.org/10.1094/MPMI.1998.11.4.277

Varma A, Malathi VG (2003): Emerging geminivirus problems: A serious threat to crop production. Ann. Appl. Biol. 142, 145–164. http://dx.doi.org/10.1111/j.1744-7348.2003.tb00240.x

Wang H, Gilbertson RL, Lucas WJ (1996): Spatial and temporal distribution of Bean dwarf mosaic geminivirus in Phaseolus vulgaris and Nicotiana benthamiana. Phytopathology 86, 1204–1214. http://dx.doi.org/10.1094/Phyto-86-1204

Wege C, Saunders K, Stanley J, Jeske H (2001): Comparative analysis of tissue tropism of bipartite geminiviruses. J. Phytopathol. 149, 359–368. http://dx.doi.org/10.1046/j.1439-0434.2001.00640.x

Zhou YC, Garrido-Ramirez ER, Sudharshana MR, Yendluri S, Gilbertson RL (2007): The N-terminus of Begomovirus nuclear shuttle protein (BV1) determines virulence or avirulence in Phaseolus vulgaris. Mol. Plant-Microbe Interact. 20, 1523–1534. http://dx.doi.org/10.1094/MPMI-20-12-1523

Zhou Y, Rojas MR, Park M, Seo Y, Lucas WJ, Gilbertson RL (2011): Histone H3 interacts and colocalizes with the nuclear shuttle protein and the movement protein of a geminivirus. J. Virol. 85, 11821–11832. http://dx.doi.org/10.1128/JVI.00082-11

Zorzatto C, Machado JPB, Lopes KVG, Nascimento KJT, Pereira WA, Brustolini OJB, Reis PAB, Calil IP, Deguchi M, Sachetto-Martins G, Gouveia BC, Loriato VAP, Silva MAC, Silva FF, Santos AA, Chory J, Fontes EPB (2015): NIK1-mediated translation suppression functions as a plant antiviral immunity mechanism. Nature 520, 679–682. http://dx.doi.org/10.1038/nature14171